Predicting apparent shear stress in prismatic compound open channels using artificial neural networks

Wenxin Huai, Gang Chen and Yuhong Zeng

ABSTRACT

The apparent shear stress acting on the vertical interface between main channel and floodplain (with and without vegetation) in prismatic compound open channels was studied using artificial neural networks (ANNs). Apparent shear stress is commonly used to quantify the transverse momentum exchange between sub-areas of the cross section, and its influencing factors include channel geometry, boundary roughness conditions and hydraulic properties of flow. In particular, if vegetations exist, the eco-characteristics of vegetation can be crucial. To mathematically describe the effect of channel symmetry, we present a new expression of width ratio through which the symmetrical and asymmetrical cross section can be distinguished. The effect of vegetation is considered using degree of submersion and the porosity (volume ratio occupied by water). Dimensional analysis was conducted to determine the mathematical formula of apparent shear stress, and seven non-dimensional parameters were selected as the influencing factors. In total, 260 sets of data (including our new experimental series conducted in a compound channel with vegetated floodplain) were used for training and testing a three-layer, feed-forward neural network with Levenberg-Marquardt (LM) as the selected training algorithm. Also, the effects of main influencing factors on the apparent shear stress were investigated.

Key words | apparent shear stress, artificial neural networks, compound channel, vegetated floodplain

Wenxin Huai
Yuhong Zeng (corresponding author)
State Key Laboratory of Water Resources and Hydropower Engineering Science,
Wuhan University,
Wuhan 430072,
China
E-mail: *yhzeng@whu.edu.cn*

Gang Chen
Yunnan Water Conservancy and Hydroelectric Survey Design and Research Institute,
Kunming 650051,
China

INTRODUCTION

Natural rivers are commonly compound channels (Figure 1), consisting of a deep main channel as the ultimate conveyer and one or two relatively shallow floodplains, which play a vital role in times of flood and are generally covered with aquatic weeds (Knight 2006). Owing to the lateral variation of geometry and roughness, the velocity in the main channel (U_c) is a magnitude larger than that in the floodplain (U_f) during flooding. Such lateral velocity difference $\Delta U = U_c - U_f$ results in a transverse momentum transfer across the main channel-floodplain interface, increasing total flow resistance as well as consuming the flow kinetic energy. That is why the traditional prediction of discharge, ignoring the main channel-floodplain interaction, does not always coincide with the corresponding measured data. As a result, quantifying the transverse momentum transfer is essential for predicting a reliable stage-discharge relationship in a compound channel.

Myers (1978) investigated compound open channel flow, and apparent shear stress was used to quantify the transverse momentum exchange between sub-areas of the cross section. Wormleaton *et al.* (1982) conducted experiments in rectangular asymmetrical and symmetrical compound channels, and the apparent shear stress was calculated as the difference between the gravity force and the boundary shear force. In this way, the apparent shear stress acting on the vertical main channel-floodplain interface, τ_a, can be quantified and various different physical meaning formulae were presented (Rajaratnam & Ahmadi 1981; Wormleaton *et al.* 1982; Knight & Hamed 1984). These formulae are generally complicated in form, and contain some unknown

doi: 10.2166/hydro.2012.193

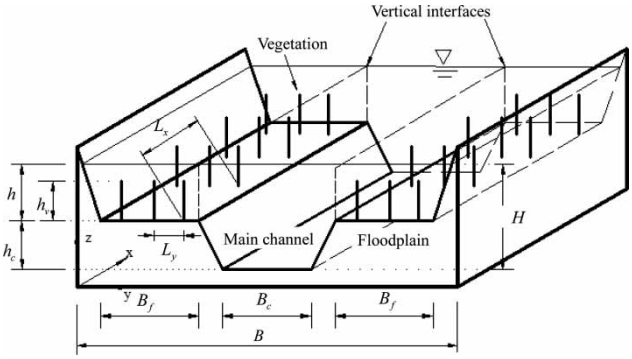

Figure 1 | Geometric parameters of compound channel.

parameters which need to be determined by experimental measuring. For example, the empirical formula for apparent shear stress presented by Knight & Hamed (1984) needs the bed shear stress to be determined in advance.

For a compound channel with vegetated floodplain, Thornton *et al.* (2000) quantified the apparent shear stress between a main channel and a vegetated floodplains based on a turbulence-based method, and an empirical formula for τ_a was presented, in which τ_a was expressed as the function of the bed shear stress, τ_b, the blockage of vegetation, velocity ratio, U_c/U_f and water depth ratio, h/H (H and h are the water depth in main channel and floodplain, respectively). During practical application, the bed shear stress, τ_b and the velocity ratio, U_c/U_f need to be determined previously.

Differing from the previously presented formulae, several quasi-theoretical formulae for estimating apparent shear stress based on Prandtl's mixing length theory have been deduced (Ervine & Baird 1982; Christodoulou 1992; Smart 1992; Bousmar & Zech 1999), in which the apparent shear stress was assumed to be proportional to ΔU^2, and the effects of geometry and roughness variation were described by an apparent friction coefficient C_{fa}. During practical application, the velocity gradient ΔU is hard to determine accurately without detailed measurements, and the uncertainty of C_{fa} with different geometry parameters and roughness conditions (Moreta & Martin-Vide 2010) increases the difficulty of application too.

Artificial neural network (ANN), as a widely applied artificial intelligent technique, has been proved to be a great success in simulating the complex non-linear process, such as hydrological analysis and prediction, river-bed scour estimation, reservoir operation and administration. For example, Minns (1996) developed an ANN-based, 'black-box' model for the rainfall-runoff process which is capable of identifying usable relationships between runoff discharges and prior rainfall depths. Azmathullah *et al.* (2005) utilized an ANN technique in predicting the characteristic parameters of a scour hole downstream of a ski-jump bucket, and the same technique was used to predict the scour below spillways (Azmathullah *et al.* 2006, 2008). Abdeen (2008) adopted an ANN technique to simulate the impacts of vegetation density, flow discharge and the operation of distributaries on the water surface profile of open channels. When it comes to compound open channel flow, the ANN technique has been successfully applied to the prediction of the hydraulics characteristics, such as integrated discharge and stage-discharge relations (Bhattacharya & Solomatine 2005; Jain 2008; Unal *et al.* 2010; Sahu *et al.* 2011).

Considering the ANN model has advantages in predicting the complex system, the authors set up an ANN-based model to estimate the apparent shear stress acted on the main channel-floodplain interface in prismatic compound channels. Furthermore, the influencing factors of the apparent shear stress were analyzed based on the ANN simulated results.

DIMENSIONAL ANALYSIS

Numerous experimental studies cited above have revealed that the major influencing factors of the apparent shear stress include the geometrical features, such as H, h, B_c, (width of the main channel), B_f (width of the floodplain), S_c (side slope) and the symmetry of the channel, and hydraulic parameters, e.g. energy slope S_0, water viscosity μ, water density ρ, the main channel roughness n_c and floodplain roughness n_f. Specially for open channel with vegetated floodplains, the ecological parameters, including plant diameter, D, vegetation height, h_v and the spaces between plants on longitudinal and transverse directions, L_x, L_y, also have effects on apparent shear stress. Therefore, the apparent shear stress can be expressed as

$$\tau_a = F(\rho, g, \mu, B_c, S_c, B_f, H, h, L_x, L_y, h_v, D, n_c, n_f, S_0) \quad (1)$$

in which F is the function symbol, and g is the gravitational acceleration.

To take the retardance effects of vegetation on the flow into consideration, we introduced two dimensionless parameters, i.e. the submergence degree, S_D and the porosity, α, and the former was defined as

$$S_D = \begin{cases} 0 & h_v = 0 \\ \dfrac{h_v}{h} & 0 < h_v \le h \\ 1 & h < h_v \end{cases} \quad (2)$$

with $S_D = 0$ denoting that there is no vegetation on the floodplains, while $S_D = 1$ means that the vegetation is emergent. The porosity (volume ratio occupied by water on the vegetated floodplain) was thus defined as

$$\alpha = \begin{cases} 1 & h_v = 0 \\ 1 - \dfrac{h_v A_v}{h L_x L_y} & 0 < h_v \le h \\ 1 - A_v/(L_x L_y) & h < h_v \end{cases} \quad (3)$$

or

$$\alpha = 1 - S_D \cdot \frac{A_v}{L_x L_y} \quad (4)$$

in which $A_v = \frac{1}{4}\pi D^2$ is the cross-sectional area of a single rod. Considering that shear velocity $u* = \sqrt{gRS_0}$, Equation (1) can be rewritten as

$$\tau_a = F_1(\alpha, \rho, u*, \mu, B_c, S_c, B_f, H, h, n_c, n_f) \quad (5)$$

where F_1 is the function symbol.

Christodoulou (1992) pointed out that the apparent shear stress is affected by the width ratio $W_r = B_c/B$ (B is the full width of the cross section). Obviously, this ratio W_r can not reflect the effects of varying cross-sectional symmetry. However, various experimental studies have validated that the apparent shear stress in an asymmetrical section is evidently larger than that in a symmetrical section, suggesting that the apparent shear stress is also affected by the cross-sectional symmetry. To obtain a generalized parameter which is capable of evaluating the symmetry of a cross section, we assumed that the transverse momentum exchange occurs only on the floodplain, linear side slope and the adjacent 75% of the main channel for compound channel. Based on the hypothesis, a new width ratio, B_r defined as $B_r = (0.75B_c + h_c S_c + B_f)/B$ was presented. Actually, for symmetrical sections, one can notice that $B_r = (0.5 + 0.25B_c/B) \le 0.75$, and for asymmetrical ones, $B_r = (1 - 0.25B_c/B) \ge 0.75$. So this parameter B_r reflects not only the impact of the width ratio, but also the effects of varying symmetry.

Ackers (1993) confirmed that apparent shear stress is strongly related to the aspect ratio $S_r = h_c/B_c = (H - h)/B_c$ and the roughness ratio $N_r = n_f/n_c$. With those dimensionless parameters, Equation (5) gives

$$\tau_a = F_2(\alpha, \rho, u*, \mu, B_r, S_c, S_r, H, h, N_r) \quad (6)$$

where F_2 is the function symbol.

Buckingham's π theorem (Sonin 2001) with H, ρ and $u*$ as the basic physical quantities was adopted to analyze Equation (6), and the apparent shear stress was expressed as following:

$$\frac{\tau_a}{\tau_b} = f\left(\alpha, B_r, S_c, S_r, N_r, D_r, \frac{u*H}{\upsilon}\right) \quad (7)$$

in which f is the function symbol, $D_r = h/H$ is the relative water depth, υ is the kinematic viscosity and $\tau_b = \rho u*^2$.

LABORATORY MEASUREMENT

Previous experimental studies have presented a wide range of observed data about apparent shear stress. These laboratory measurements, experimenting on symmetrical or asymmetrical channels with non-vegetated main channel and/or vegetated floodplains, were conducted in either small-scale flumes or a large-scale Flood Channel Facility (FCF) under uniform conditions. As the data for compound open channels with vegetated floodplains are not sufficient, two series of experiments were reproduced in a physical model of a straight, rectangular, asymmetrical compound channel constructed in the Hydraulics Laboratory of Wuhan University. The channel was assembled in a glass recirculating flume 0.5 m wide and 20 m long, and the bed slope was fixed as 0.4%. Water was pumped from an underground reservoir to a 20 m high water tank, and then overflowed into the flume through a wave suppressor. The discharge was recorded by

an electric magnetic valve with an accuracy of 0.1 l s^{-1}, and the water surface was adjusted to be parallel to the channel bed by a tail-gate to keep the flow uniform.

The widths of the main channel and floodplain were both 0.25 m, and the main channel was 0.125 m deeper than the floodplain. Holes of 6 mm diameter with longitudinal and lateral spacing distances of 0.05 m were drilled on the floodplain bed, in which the 0.125 m tall steel bars with a diameter of 6 mm were inserted to simulate rigid, rod-like vegetation without foliage. The 3D flow velocities were measured by a 16 MHz Micro ADV system equipped with an upward probe and a downward probe. For each run three cross-sections with a space of 2 m were measured, and the vertical interval of measuring on the main channel was 2 cm, and that on the floodplain was 1 cm. Two series with unsubmerged (O-s1 in Table 1) and submerged vegetation (O-s2 in Table 1) on the floodplain were conducted. For each series, four non-staggered vegetation arrays with spacings $L_x \times L_y =$ 0.05×0.05 m, 0.05×0.1 m, 0.1×0.05 m, and 0.1×0.1 m, and two staggered arrays with spacings $L_x \times L_y = 0.05 \times 0.1$ m and 0.1×0.1 m were adopted. A summary of the tests is listed in Table 1.

Similar to Thornton *et al.* (2000), the apparent shear stress was derived by the relationship between shear stress and turbulence,

$$\tau_a = \rho \overline{u'_x u'_y} \tag{8}$$

where u'_x = fluctuation of velocity in the x direction and u'_y = fluctuation of velocity in the y direction.

ANN MODEL FOR APPARENT SHEAR STRESS

Network architecture

A three-layer (one input layer, one hidden layer and one output layer) feed-forward ANN model was adopted.

Table 1 | Summary of experimental parameters

Test series	Q (L/s)	H (m)	h (m)	B (m)	D_r
O-s1 (unsubmerged)	22.9	0.212	0.087	0.50	0.410
O-s2 (submerged)	40.1	0.305	0.180	0.50	0.590

Feedforward neural networks have been applied successfully in many different problems, since the input signal propagates through the network in a forward direction, layer by layer and easy to be handled (Daliakopoulos *et al.* 2005). The Levenberg-Marquardt (LM) algorithm, is often characterized as more stable and less easily trapped in local minima than other optimization algorithms (Bezerra *et al.* 2008), so LM was selected to optimize the adjustable parameters of the weights and biases. The training was carried out using the following parameters: (1) constant learning rate = 0.4; (2) constant momentum factor = 0.3; and (3) mean square error target = 10^{-6}.

The observed data (totally 260 sets of data, with N the total experimental runs of each series) listed in Table 2 were divided randomly into two groups: 80% of which as the training set and the remainder as the testing set. The training set, consisting of input and known output data, serves the ANN training to determine a reasonable set of weights. Training data were scaled in the range [0.1, 0.9] to make weight estimation more feasible. The simulation was realized by using the ANN toolbox of Matlab 7.6.

The objective of the training procedure is to find a set of possible weights that will enable the network to produce the prediction as similar as possible to the known experimental output data. This is achieved by minimizing the cost function E, which is the root mean square error as shown below:

$$E = \sqrt{\frac{1}{M}\sum_{i=1}^{M}\left((\tau_a)_{m_i} - (\tau_a)_{p_i}\right)^2} \tag{9}$$

where M is the number of measurements, $(\tau_a)_{m_i}$ is the measured apparent shear stress and $(\tau_a)_{p_i}$ is the predicted result.

A suitable number of the hidden neurons can avoid over-fitting, and allows one to control the accuracy level with respect to the noise level (Giustolisi & Laucelli 2005). Here the number of nodes in the hidden layer was determined through trial and error method (Bezerra *et al.* 2008), and the optimal node with the minimal E was determined as 8. Therefore, the architecture of the three-layer neural network adopted has seven input nodes, eight hidden nodes and one output node (Figure 2).

Table 2 | Main parameters of tests

		Geometrical parameters					Test conditions			
Sources	**Series ref.**	B_f (m)	S_c	S_r	B_c (m)	B_r	N_r	S_o (%)	α	N
Wormleaton & Merrett (1990)	W-SA	0.46 × 2	Rect.(0H:1V)	0.414	0.29	0.56	1.00	0.43	1.00	7
	W-SB						1.40			6
	W-SC						1.70			8
	W-SD						2.10			8
Noutsopoulos & Hadjipanos (1983)	NH-A1	0.425 × 2	Rect.(0H:1V)	0.500	0.15	0.54	1.00	1.5	1.00	5
	NH-A2	0.325 × 2		0.485		0.55				6
	NH-A4	0.225 × 2		0.500		0.56				5
Knight & Demetriou (1983)	KD-S3	0.229 × 2	Rect.(0H:1V)	0.500	0.15	0.56	1.00	0.966	1.00	6
	KD-S2	0.152 × 2				0.58				6
	KD-S1	0.076 × 2				0.63				6
Knight *et al.* (1983)	K-S3	0.229 × 1	Rect.(0H:1V)	0.500	0.15	0.90	1.00	0.966	1.00	7
Knight & Hamed (1984)	KH-R4	0.229 × 2	Rect.(0H:1V)	0.500	0.15	0.56	1.09 ~ 1.14	0.966	1.00	6
	KH-R5						1.19 ~ 1.31			6
	KH-R6						1.33 ~ 1.62			6
	KH-R7						1.71 ~ 2.44			6
	KH-R8						2.12 ~ 3.94			6
	KH-R9						2.47 ~ 6.23			6
Prinos & Townsend (1984)	PT-A1	0.203 × 2	Trap.(1H:2V)	1.070	0.10	0.54	1.00	0.966	1.00	6
	PT-B1						1.27			6
	PT-C1						1.64			6
	PT-D1						2.00			6
	PT-A2	0.305 × 2		0.473	0.22	0.56	1.00			6
	PT-B2						1.27			6
	PT-C2						1.64			6
	PT-D2						2.00			6
Large-scale FCF (www.flowdata.bham.ac.uk/fcf-data.shtml)	FCF-s1	4.10 × 2	Trap.(1H:1V)	0.104	1.45	0.54	1.00	1.027	1.00	7
	FCF-s2	2.25 × 2		0.103		0.56				8
	FCF-s3	0.75 × 2		0.110		0.61				7
	FCF-s6	2.25 × 1		0.107	0.75	0.94				8
	FCF-s7	2.25 × 2		0.200	1.41	0.56	1.16 ~ 3.66			8
	FCF-s8	2.25 × 2	Rect.(0H:1V)	0.107		0.56	1.00			8
	FCF-s10	2.25 × 2	Trap.(2H:1V)	0.107		0.55	1.00			8
Atabay *et al.* (2004)	A-SR	0.407 × 2	Rect.(0H:1V)	0.126	0.40	0.58	1.00	2.024	1.00	12
Atabay *et al.* (2005)	A-AR	0.407 × 1	Rect.(0H:1V)	0.126	0.40	0.88	1.00	2.024	1.00	12
Thornton *et al.* (2000)	T-s1	0.76 × 1	Rect.(0H:1V)	0.326	0.46	0.91	1.00	1.72 ~ 4.86	1.00	4
	T-s2						1.00	1.72 ~ 6.49	0.94 ~ 0.98	12
Our experiments	O-s1	0.25 × 1	Rect.(0H:1V)	0.500	0.25	0.88	1.00	0.4	0.989 ~ 0.997	6
	O-s2								0.992–0.998	6

Evaluation of the ANN performance

The training data set was used to adjust the weights of all connecting nodes until the desired error level was reached. The ANN performance can be evaluated using the correlation coefficient R which is defined by:

$$R = \frac{\sum_{i=1}^{M}\left[(\tau_a)_{m_i} - \overline{(\tau_a)_m}\right]\left[(\tau_a)_{p_i} - \overline{(\tau_a)_p}\right]}{\sqrt{\sum_{i=1}^{M}\left[(\tau_a)_{m_i} - \overline{(\tau_a)_m}\right]^2}\sqrt{\sum_{i=1}^{M}\left[(\tau_a)_{p_i} - \overline{(\tau_a)_p}\right]^2}} \quad (10)$$

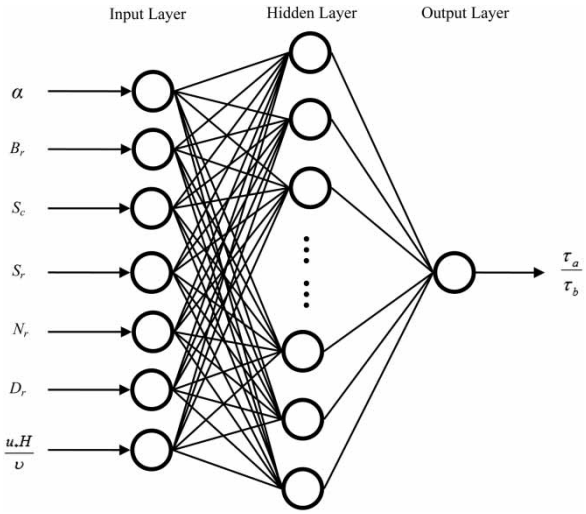

Figure 2 | ANN architecture for the prediction of apparent shear stress.

where $(\tau_a)_{m_i}$ is the observed τ_a, $\overline{(\tau_a)}_m$ is the average observed $(\tau_a)_{p_i}$; $(\tau_a)_{p_i}$ is the ANN-predicted τ_a, and $\overline{(\tau_a)}_p$ is the average ANN-predicted τ_a.

For this work, a correlation coefficient $R = 0.9997$ was achieved after about 1,680 times training, and the high R shows that a well-trained network has been achieved. The predicted results of the ANN-based model were compared with the observed data in Figure 3.

With the well-trained network, the testing data set was used to evaluate the performances of the model. A correlation coefficient $R = 0.997$ was obtained which means the apparent shear stress predicted by our model coincides with the observed data. The comparison between the predicted and measured value is shown in Figure 4.

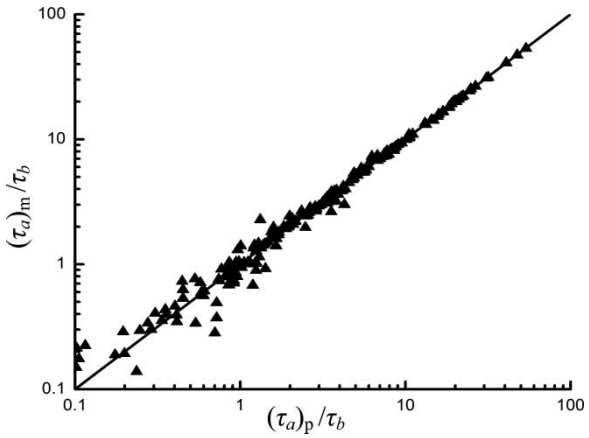

Figure 3 | Measured and predicted apparent shear stress (normalized by τ_b) in the training period.

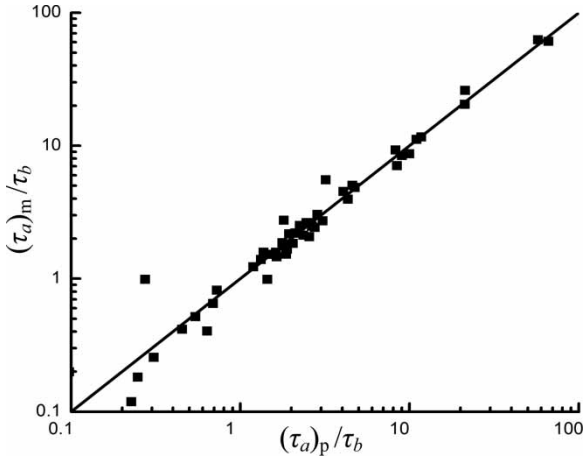

Figure 4 | Measured and predicted normalized apparent shear stress in the testing period.

APPLICATION AND ANALYSIS

The analysis of the weight and threshold matrixes, based on the results of training, was conducted to determine the decisive factors in predicting the apparent shear stress. The present work focused on utilizing the model presented in the previous section to analyze the influence of those main π items in Equation (7) on the apparent shear stress.

Influence of the relative water depth and the roughness ratio

A number of laboratory observations have validated that the increase of the relative water depth results in a decrease of apparent shear stress. The representative example is that performed by Knight & Hamed (1984), who conducted six series of experiments in a rectangular symmetrical channel with rough floodplains. The ANN predicted apparent shear stresses and measured data for the six series KH-R4–R9 (details in Table 2) with different roughness ratios, N_r =1.0, 1.2, 1.5, 2.0, 2.5 and 3.0, respectively, and are plotted against D_r in Figure 5. Clearly, the apparent shear stress increases with the increase of the roughness ratio, and decreases with the increase of relative water depth.

Further work proved the above conclusion. The geometrical and hydraulic parameters of series K-S3 (Knight *et al.* 1983, details in Table 2) were adopted, except that the roughness ratio was set to vary from 1 to 4 in a 0.02

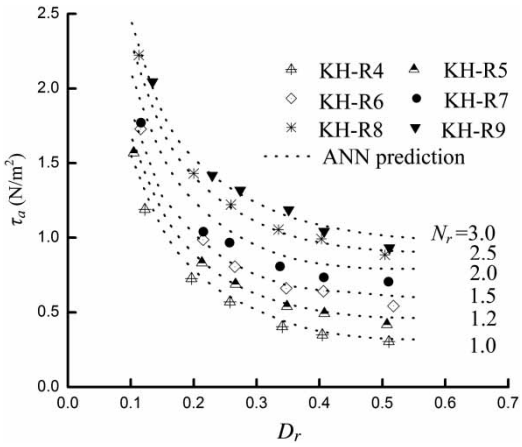

Figure 5 | Observed and predicted τ_a varied with different relative water depths and roughness ratios.

increment, and the result indicated that the apparent shear stresses have a linear relationship with the roughness ratio. By curve fitting we got $\tau_a = 0.20967 + 0.48505N_r$ with a correlation coefficient $R = 0.9998$.

Influence of the width ratio

The geometrical and hydraulic parameters of series K-S3 in Table 2 were used for analysis, except that the floodplain width was set to vary from 0.01 to 0.30 m in a 0.01 m increment to make the width ratio fall into a certain range. The ANN predictions of how apparent shear stress varied with different width ratio are shown in Figure 6. In more detail, $B_r \in [0.55, 0.72]$ for symmetric sections (the left half of Figure 6) and $B_r \in [0.77, 0.92]$ for asymmetric sections (the right half of Figure 6).

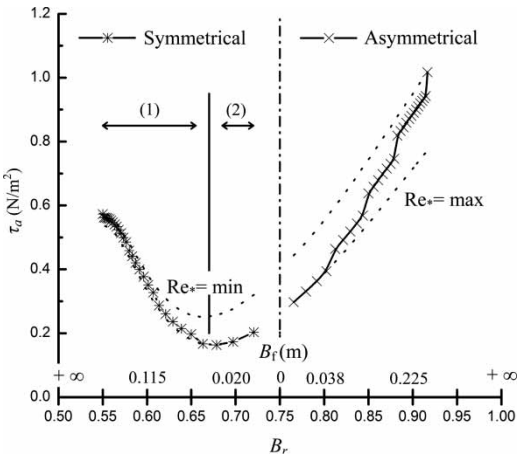

Figure 6 | Variation of apparent shear stress with the width ratio ($B_c = 0.15$ m and $h_c = 0.076$ m).

For symmetrical sections in Figure 6, a marked inflexion point appeared around $B_r = 0.66$, partitioning the $\tau_a - B_r$ curve into two regimes. In the first regime, the apparent shear stress sharply decreases with the increase of the width ratio, while it slowly increases in the second regime as the width ratio increases, or the floodplain width decreases. However, the reason for this phenomenon is still not clear and demands more future investigations. The insufficient training of the data set within the range $B_r \in [0.66, 0.72]$ may be a reason for the inflexion. And the combined mean of B_r (width ratio and cross-sectional symmetry) can increase the complexity of analysis too. For asymmetrical sections, the overall trend of variation for the apparent shear stress curve is ascending with the increase of width ratio. Note that apparent shear stress in an asymmetrical section is larger than that in a symmetrical section of the same floodplain width for this analysis.

The Reynolds number $\mathrm{Re}* = u*H/\upsilon$ also varies with the variation in floodplain width. Therefore, to make a contrast, we predicted and plotted how the apparent shear stress varied with ratio of width under two constant Reynolds numbers, one is the maximum Reynolds number of the runs (for the symmetrical one, $\mathrm{Re}_{*\max} = 7{,}287$; and for the asymmetrical one, $\mathrm{Re}_{*\max} = 8{,}162$) and the other is the minimum (symmetrical, $\mathrm{Re}_{*\min} = 3{,}764$; asymmetrical, $\mathrm{Re}_{*\min} = 3{,}404$). From Figure 6, the conclusion can be made that the effect of Reynolds number on the apparent shear stress is not obvious, since the flow is already a fully turbulent one.

CONCLUSIONS

Experiments in a straight, asymmetrical compound channel with simulated rigid vegetation on the floodplain were conducted, and the apparent shear stress at the main channel-floodplain interface was quantified by the local turbulence at the interface. With the measured and collected data from literature, a three-layer, feed-forward ANN model with LM as the optimization procedure was successfully constructed to predict the apparent shear stress in prismatic symmetric/asymmetric compound channels with

non-vegetated/vegetated floodplains. As Thornton *et al.* (2000) mentioned, those commonly used empirical formulae obtained through multiple regression methods were only applicable for given boundary conditions, while the ANN model is a general model which is able to predict the combined effect of channel geometry, the vegetation retardance, roughness conditions, etc., on the apparent shear stress. From this aspect, the ANN model is a good substitute when direct measuring is not achievable. For this study, the analysis of affecting factors of apparent shear stress based on the ANN predictions is sound, but further analysis on those parameters such as the newly presented width ratio needs more detailed laboratory measuring.

ACKNOWLEDGEMENTS

This work was financially supported by the Natural Science Foundation of China (Nos 10972163, 50979078), and the Program for New Century Excellent Talents in the University of China (No. NCET-11–0393). The authors would like to thank the anonymous reviewers for providing constructive suggestions.

REFERENCES

Abdeen, M. A. M. 2008 Predicting the impact of vegetations in open channels with different distributaries' operations on water surface profile using artificial neural networks. *Journal of Mechanical Science and Technology* **22**, 1830–1842.

Ackers, P. 1993 Flow formulae for straight two-stage channels. *Journal of Hydraulic Research* **31**, 509–531.

Atabay, S., Knight, D. W. & Seckin, G. 2004 Influence of a mobile bed on the boundary shear in a compound channel. In: *River Flow 2004* (M. Greco, A. Carravetta & R. Della Morte, eds). *Proc. 2nd Intl Conf. on Fluvial Hydraulics*, Napoli, Italy, Balkema, The Netherlands, pp. 337–345.

Atabay, S., Knight, D. W. & Seckin, G. 2005 Effects of overbank flow of fluvial sediment transport rates. *Proc. ICE, Water Management* **158**, 25–34.

Azmathullah, H. Md., Deo, M. C. & Deolalikar, P. B. 2005 Neural networks for estimation of scour downstream of a ski-jump bucket. *Journal of Hydraulic Engineering, ASCE* **131**, 898–908.

Azmathullah, H. Md., Deo, M. C. & Deolalikar, P. B. 2006 Estimation of scour below spillways using neural networks. *Journal of Hydraulic Research* **44**, 61–69.

Azmathullah, H. Md., Deo, M. C. & Deolalikar, P. B. 2008. Alternative neural networks to estimate the scour below spillways. *Advances in Engineering Software* **39**, 689–698.

Bezerra, E. M., Bento, M. S., Rocco, J. A. F. F., Iha, K., Lourenço, V. L. & Pardini, L. C. 2008 Artificial neural network (ANN) prediction of kinetic parameters of (CRFC) composites. *Computational Materials Science* **44**, 656–663.

Bhattacharya, B. & Solomatine, D. P. 2005 Neural networks and M5 model trees in modelling water level–discharge relationship. *Neurocomputing* **63**, 381–396.

Bousmar, D. & Zech, Y. 1999 Momentum transfer for practical flow computation in compound channels. *Journal Hydraulic Engineering* **125**, 696–706.

Christodoulou, G. C. 1992 Apparent shear stress in smooth compound channels. *Water Resource Management* **6**, 235–247.

Daliakopoulos, I. N., Coulibaly, P. & Tsanis, I. K. 2005 Groundwater level forecasting using artificial neural networks. *Journal of Hydrology* **309**, 229–240.

Ervine, D. A. & Baird, J. I. 1982 Rating curves for rivers with overbank flow. *Proceedings of the Institution of Civil Engineers* **73**, 465–472.

Giustolisi, O. & Laucelli, D. 2005 Improving generalization of artificial neural networks in rainfall–runoff modelling. *Hydrological Sciences Journal* **50**, 439–457.

Jain, S. K. 2008 Development of integrated discharge and sediment rating relation using a compound neural network. *Journal of Hydrologic Engineering* **13**, 124–131.

Knight, D. W. 2006 River flood hydraulics: theoretical issues and stage-discharge relationships. In: *River Basin Modelling for Flood Risk Mitigation* (D. W. Knight & A. Y. Shamseldin, eds). Taylor & Francis, London, pp. 301–334.

Knight, D. W. & Demetriou, J. D. 1983 Flood plain and main channel flow interaction. *Journal of Hydraulic Engineering* **109**, 1073–1092.

Knight, D. W., Demetriou, J. D. & Hamed, M. E. 1983 Hydraulic analysis of channels with floodplains. *Proc. Intl. Conf. Hydraulic Aspects of Floods and Flood Control*, BHRA Fluid Engineering, Bedford, pp. 129–144.

Knight, D. W. & Hamed, M. E. 1984 Boundary shear in symmetrical compound channels. *Journal of Hydraulic Engineering* **110**, 1412–1430.

Minns, W. 1996 Extended rainfall-runoff modelling using artificial neural networks. In: *Hydroinformatics '96. Proc 2nd. Int. Conf.* (A. Muller, ed.), Taylor & Francis, Zurich, pp. 207–213.

Moreta, P. J. M. & Martin-Vide, J. P. 2010 Apparent friction coefficient in straight compound channels. *Journal of Hydraulic Research* **48**, 169–177.

Myers, W. R. C. 1978 Momentum transfer in a compound channel. *Journal of Hydraulic Research* **16**, 139–150.

Noutsopoulos, G. & Hadjipanos, P. 1983 Discharge computations in compound channels. *Proc. 20th IAHR Congress*, Moscow, pp. 173–180.

Prinos, P. & Townsend, R. D. 1984 Comparison of methods for predicting discharge in compound open channels. *Advances in Water Resources* **7**, 180–187.

Rajaratnam, N. & Ahmadi, R. 1981 Hydraulics of channels with flood-plains. *Journal of Hydraulic Research* **19**, 43–60.

Sahu, M., Khatua, K. K. & Mahapatra, S. S. 2011 A neural network approach for prediction of discharge in straight compound open channel flow. *Flow Measurement and Instrumentation* **22**, 438–446.

Smart, G. M. 1992 Stage-discharge discontinuity in composite flood channels. *Journal of Hydraulic Research* **30**, 817–833.

Sonin, A. A. 2001 *The Physical Basis of Dimensional Analysis*. 2nd edition, Department of Mechanical Engineering MIT, Cambridge, MA.

Thornton, C. I., Abt, S. R., Morris, C. E. & Craig Fischenich, J. 2000 Calculating shear stress at channel-overbank interfaces in straight channels with vegetated floodplains. *Journal of Hydraulic Engineering, ASCE* **126**, 929–936.

Unal, B., Mamak, M., Seckin, G. & Cobaner, M. 2010 Comparison of an ANN approach with 1-D and 2-D methods for estimating discharge capacity of straight compound channels. *Advances in Engineering Software* **41**, 120–129.

Wormleaton, P. R., Allen, J. & Hadjipanos, P. 1982 Discharge assessment in compound channel flow. *Journal of the Hydraulics Division* **108**, 975–994.

Wormleaton, P. R. & Merrett, D. J. 1990 An improved method of calculation for steady uniform flow in prismatic main channel/flood plain sections. *Journal of Hydraulic Research* **28**, 157–174.

First received 7 December 2011; accepted in revised form 25 May 2012. Available online 1 September 2012